MINERALOGICAL MAGAZINE, VOL. 45, 1982, PP. 193–200

# Pyroxene fractionation in ferrobasalts from the Galapagos Spreading Centre*

I. D. MUIR

Department of Earth Sciences, University of Cambridge

AND

D. A. MATTEY

Department of Geophysics, University of Hawaii, Honolulu

ABSTRACT. The significance of metastable and equilibrium pyroxene fractionation trends in tholeiitic magmas is discussed, and the development of sector zoning and skeletal growth are considered in relation to Nakamura's (1973) hypothesis of protosites on growing clinopyroxene crystal surfaces. At the Galapagos Spreading Centre (GSC) basalts and ferrobasalts investigated behave paradoxically in that the slower-cooled basalts follow the quench trend while the faster-cooled ferrobasalts define a much closer approach to the equilibrium trend.

It is concluded that under metastable conditions fractionation trends in Ca-rich pyroxenes may be strongly influenced by textural features such as cotectic crystallization of plagioclase and the onset of liquid immiscibility, the latter leading to the development of strongly Fe-enriched ferroaugites. Even under plutonic conditions metastable crystallization can develop and severely reduce the pyroxene miscibility gap. A model for metastable crystallization is presented. These considerations are then addressed to the remarkable correspondence of the Skaergaard and Thingmuli pyroxene fractionation trends.

THE problem of effecting distinctions between equilibrium and metastable pyroxene fractionation trends in basic magmas has been much disputed during the last fifty years and is not yet fully resolved. One of the most forward-looking of the early analyses was that of Wager and Deer in their Memoir on the Skaergaard Intrusion (1939, pp. 240–61). They pointed out that in the early stages both trends were similar, with the augites being progressively depleted in Ca; this lead to the development of subcalcic augites under volcanic conditions. Under plutonic conditions, however, two separate pyroxene phases are developed, and in the augite series a trend towards ferroaugite sets in. Muir (1954) developed a model to explain the miscibility gap under equilibrium conditions between co-existing Ca-rich and Ca-poor pyroxenes in terms of the intersection of the crystallization surface with the pyroxene solvus.

The trend under extrusive conditions was re-examined by Muir and Tilley (1964) who pointed out that the early replacement of Ca by Fe led first to the development of a subcalcic augite and in extreme cases to ferropigeonite as well. Under volcanic conditions the groundmass pyroxenes of many tholeiitic basalts clearly fell well within the pyroxene miscibility gap and must be regarded as metastable. For the augite series these authors distinguished between an 'equilibrium trend', well shown by Skaergaard Intrusion and by thick dolerite sills (McDougall, 1962), and a 'quench trend' represented by the crystallization of tholeiitic basaltic magmas under extrusive conditions. In the Ca-poor series of pyroxenes a single trend leading to Fe enrichment with very minor Ca enrichment in the middle stages is found, although the intersection with the solvus appears to be slightly reduced under volcanic conditions (fig. 1).

Muir and Tilley's observations were disputed by Carmichael (1967) who pointed out that at Thingmuli in Iceland, although a single pyroxene phenocryst phase, augite, was present in the basalts, two coexisting series of pyroxenes occurred in the groundmass. The phenocryst trend closely follows that of Skaergaard, but this trend is parallelled by that of the groundmass pyroxenes, although with a distinctly narrower miscibility gap (fig. 1). Carmichael suggested that the Thingmuli trends might be explained by the more Fe-rich nature of the Icelandic magmas, which by reducing both temperature and viscosity could perhaps encourage equilibrium assemblages. He concluded with this

* Department of Earth Sciences, University of Cambridge, Contribution No. 195.

profound observation: 'Thus the distinction made by Muir and Tilley between the metastable and quench pyroxene trend of the volcanic effusives on the one hand and the intratelluric or equilibrium trend on the other (e.g. Skaergaard) cannot be related solely to the rate of cooling, and the term "quench" in this context is possibly best forgotten.'

This advice does not seem to have been heeded, for a number of later works (e.g. Evans and Moore, 1968; Nakamura and Kushiro, 1970; Yamakawa, 1971) appear to substantiate the distinction, a particularly striking example being cited by Smith and Lindsley (1971) from a particularly thick flow (95 m) of Picture Gorge basalt where the coarse-grained centre follows the early part of the Thingmuli phenocryst trend, while in the chilled margins the quench trend is followed. The problem in mildly undersaturated and tholeiitic magmas was discussed by Barberi *et al.* (1971) who concluded that the fractionation path of Ca-rich clinopyroxenes under effusive conditions is controlled by a number of chemical and physical factors that include, as well as initial temperature and degree of undercooling of the host melt, the nature and concentration of volatiles, $f_{O_2}$, and the cotectic crystallization of other minerals, particularly plagioclase.

If early separation of calcic plagioclase in significant amounts can be induced this will deplete the melt in the Ca-Tschermak component and cause the augite that subsequently crystallizes to fractionate towards subcalcic compositions. This effect is often seen in tholeiites, but in the Erta'Ale Range in N. Afar, Ethiopia, Barberi *et al.* (1970, 1971) have described convincing examples of mildly alkaline basaltic magmas that have fractionated under unusually low $f_{O_2}$ conditions to produce subcalcic augites, and in one case, a ferrobasalt, with solvus intervention, Fe-rich pigeonite as well.

Further information on metastable pyroxene fractionation trends comes from the study of sector-zoned crystals. Here significantly different compositions may be deposited simultaneously on the growing surfaces of different crystal faces under supercooled conditions (Hollister and Gancanz, 1971; Boyd and Smith, 1971). The most spectacular examples come from the Lunar Apollo 12 suite where euhedral phenocrysts have cores (sometimes hollow) of relatively homogeneous pigeonite zoned outwards towards subcalcic augite on the {100} faces with a very small miscibility gap. Continuous zoning to Fe-enriched pigeonite occurs on {010}, while on {110} the pigeonite core is sharply mantled epitaxially by a zone of moderately subcalcic augite, with one major (100 $\mu$m) and a

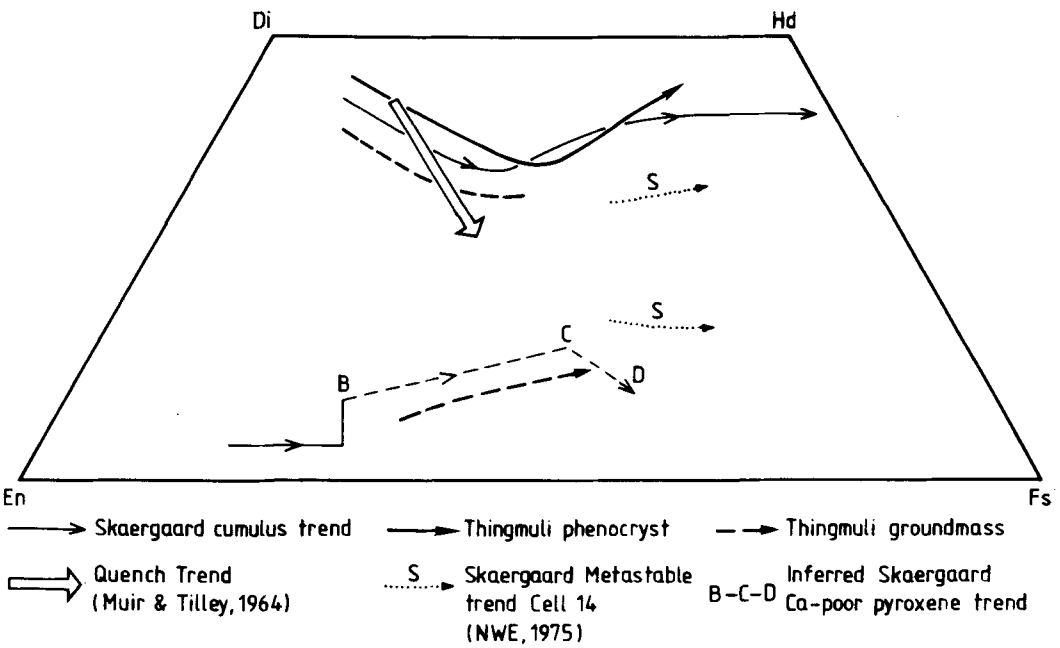


FIG. 1. Comparison of Skaergaard equilibrium (Brown, 1957; Brown and Vincent, 1963) trends with those of Thingmuli; average compositions for phenocrysts (heavy line) and groundmass compositions (dashed lines) after Carmichael (1967). Also shown is the Hawaiian quench trend (after Muir and Tilley, 1964) and the metastable trend in the Skaergaard trough band intercumulus cells (Nwe, 1975). BCD Equilibrium Skaergaard Ca-poor pyroxene trend (Muir in Gay *et al.*, 1971; Nwe, 1957); BC inverted pyroxenes; CD pigeonites.

number of minor ($\sim$ 10 $\mu$m) recurrences of a more Fe-rich pigeonite. Abrupt changes of the type seen in the minor recurrences, featuring pigeonite in augite and vice versa, are difficult to explain except as kinetic problems in which it is energetically more favourable for pigeonite or augite to be deposited on a suitable existing pyroxene substrate rather than to form separate nuclei, a feature commonly observed in dolerites. Boyd and Smith correlate the formation of the major pigeonite band with the onset of cotectic crystallization of plagioclase ($An_{90}$).

For the Apollo 11 suite Murase and McBirney (1970) were able to show that viscosities were likely to be more fluid than Columbia River basalt by an order of magnitude. In these very fluid lunar melts diffusion was rapid and fractional crystallization was better able to keep pace with cooling.

On a much more modest scale this type of zoning has been encountered in some terrestrial basalts and dolerites (Nakamura, 1973). It also appears to be developed mildly in ocean-floor basalts when a subophitic texture is present (Thompson and Humphris, 1980). Here again we note the tendency for subgrains of pigeonite to nucleate on the {110} faces of augite in locations contiguous to plagioclase.

Nakamura (1973) has used the concept of protosites on growing crystal surfaces to explain sector zoning and has pointed out how the increase in free energy associated with the entry of Mg and Fe atoms into the incompletely coordinated $M(1)$ and $M(2)$ protosites above the limit of the solvus composition on a fast-growing {100} surface is likely to be significantly less than if they were introduced into a completely coordinated $M(2)$ site; but this tolerance does not extend to {010}. The situation on {110} appears to be intermediate between these two extremes and in high-temperature pyroxenes where both phases have the $C2/c$ structure (Prewitt *et al.*, 1970) it is probable that the extent of structural mismatch between the phases is sufficiently small to permit easy epitaxial growth on {110} but not on {010}. Such considerations, together with the compositions involved, persuaded Boyd and Smith that relations in the {110} sectors where there is a sharp compositional break, most closely approximated to equilibrium crystallization. In cases of skeletal growth where a dominant zone axis is involved it is probable that metastable relations will profoundly influence pyroxene fractionation trends.

### *The GSC ferrobasalts*

It has been known for some time that ferrobasalts, rocks with strong tholeiitic affinities in which the ratio of iron to magnesia, calculated as FeO*/MgO, is greater than 2, are very common along the fast-spreading, non-rifted ridges of the eastern Pacific. Nowhere are they more common than at the Galapagos Spreading Centre (GSC), some 300 km to the north of the Galapagos Islands. Here the unscheduled drilling programme on DSDP Leg 54 provided the first stratigraphic sampling of young basaltic rocks from this region. Short cores were obtained from two sites at 86° W, 424 and 425, respectively 22 km south and 62 km north of the spreading axis (Mattey and Muir, 1980). Three distinct chemical types of basalt, all somewhat evolved, occur at Site 425, but only one, ferrobasalt with about 13.5% FeO* and 6.5% MgO, was found in all four holes drilled at Site 424. Here all the rocks recovered are plagioclase–clinopyroxene–phyric ferrobasalts with very uniform chemistry. The principal variation encountered concerns degree of crystallinity, specimens varying from coarse to fine grained and even to glassy, sometimes within the scale of a single thin section. Pillow structures appear to be present, but the cooling units are very thin, mostly in the range 0.2–2 m in thickness. There appear to be numerous flows in this locality, each of very limited extent, but all derived from the same magma chamber.

Most specimens carry sparse phenocrysts of calcic plagioclase ($An_{76-50}$) with complex zoning; typically they tend to occur in clusters associated with clinopyroxene and titanomagnetite (glomerophyric texture). Rare crystals of olivine ($Fo_{76-72}$) are occasionally present. Where a subophitic texture is developed, a tendency towards sector zoning can sometimes be detected in the clinopyroxene and an occasional sub-grain of pigeonite can also be encountered immediately adjacent to plagioclase; as noted earlier, the plane of junction of the two pyroxenes often appears to be {110}. The groundmass is composed of more Fe-rich pyroxenes, plagioclase ($An_{60-50}$) titanomagnetite, and what at first appears to be an interstitial Fe-rich glass, still relatively fresh, but now devitrified. Closer examination of this glassy region reveals evidence that extensive liquid immiscibility has developed at a late stage. Two glasses appear to have been present; the dominant one Fe- and Ti-rich and silica-poor, has now recrystallized to an assemblage of dark-brown pyroxene, elongated skeletal crystals of titanomagnetite, and an andesine. From the conjugate silica-rich liquid the same phases plus a silica mineral have crystallized.

The less fractionated basalts of Site 425 with Fe*/MgO ratios 1.1–1.6, are generally similar petrographically to the ferrobasalts but are less

* Total iron oxides calculated as FeO.

fresh and derive from much thicker flow units. Indeed some may come from sills. Analyses of all these basalt types are given by Mattey and Muir (1980).

### *The clinopyroxenes*

*Phenocrysts* are occasionally found in the Site 424 ferrobasalts but they are more abundant at Site 425; the compositional ranges found are illustrated by the encircled areas shown on fig. 2. The principal variation is in the Ca content at a relatively constant Fe/Mg ratio. Much of the variation is produced by a somewhat patchy concentric zoning resulting in the rims being less calcic, and usually poorer in $Al_2O_3$ and $Cr_2O_3$ than the cores. There are significant differences in over-all composition between the phenocrysts from the two sites, those from the basalts being typically Ca- and Mg-rich augites with significant amounts of $Cr_2O_3$ (0.4–1%) but relatively low in $TiO_2$ (0.2–0.4%). Their 100 Mg/(Mg+Fe) ratios vary from 86 to 83. Those from the ferrobasalts are less magnesian augites with this ratio close to 78; they are poorer in $Cr_2O_3$ and slightly richer in $TiO_2$ and $Na_2O$ than are the basalt phenocrysts (Table I, anals. 1–4).

*Groundmass pyroxenes*, in contrast to the phenocrysts, display a considerable range in composition, those from the ferrobasalts being generally richer in FeO, $TiO_2$, $Al_2O_3$, MnO, $Na_2O$, and poorer in $Cr_2O_3$ (Table I, anals. 5–10). At Site 425 there is a moderate variation in Mg ratio (82–60) but the principal variation concerns Ca which varies from $Ca_{44}$ to $Ca_{22}$. Occasional grains of pigeonite are present but ferroaugites are rare. Analyses from the ferrobasalts reveal a much greater range of Mg ratio (75–40) while Ca varies to a lesser extent (most $Ca_{40-30}$). Thus the fractionation trend is one of relatively constant Ca through Fe-rich augite to ferroaugite as in many plutonic intrusions.

In the rocks investigated here we have the paradox of the demonstrably slower-cooled samples from Site 425 being dominated by the 'quench trend', while the more rapidly cooled ferrobasalts of Site 424 display a much closer approach to the 'equilibrium trend'. In order to investigate this matter further, a Site 424 ferro-

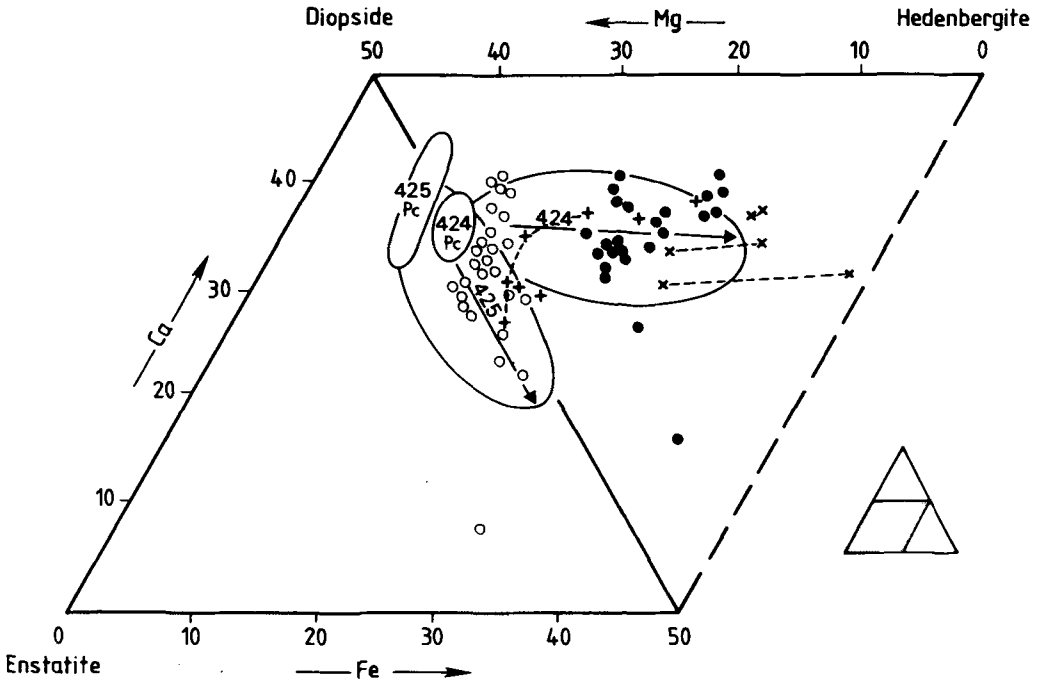


FIG. 2. 425Pc and 424Pc, range of phenocryst compositions encountered at GSC Sites 425 and 424 respectively. Arrows show generalized fractionation trends for groundmass pyroxenes for which limits of variation are indicated by elliptical areas. Also shown are groundmass pyroxenes from Section 424-6-1 (piece 10): closed circles, granular pyroxenes of mesostasis; open circles, ophitic grains; crosses, feathery extensions of ophitic pyroxenes extending into Fe-rich formerly glassy regions. Dotted lines link analyses from same crystal and indicate how clinopyroxenes become enriched in Fe and Ca as they grow into glassy regions (after Mattey and Muir, 1980, but with additional data).

basalt displaying the extreme variations in texture mentioned above was studied in more detail. The groundmass pyroxene of this sample was of two types.

1. *Ophitic clinopyroxene.* This forms relatively coarsely crystalline areas surrounded by a mesostasis composed of approximately equal areas of finely crystalline material and devitrified glasses. The ophitic pyroxene forms optically continuous plates up to 1 mm in diameter.

2. *Granular clinopyroxene.* Here groups of small overlapping grains float in large patches of mesostasis which also contain granular or skeletal titanomagnetite, and microlites of skeletal plagioclase. Some of the clinopyroxenes embedded in the mesostasis have a coarser morphology and some have feathery extensions. Some are twinned while others display patchy or undulose extinction.

Seventy-five analyses including both types of pyroxene are plotted in fig. 2 and two representative analyses are listed in Table I, anals. 9 and 10). The range of pyroxene compositions encountered in this single sample exceeds the combined variation of the pyroxenes in all the other GSC rocks analysed in this study. But analyses of ophitic and granular types clearly fall into two groups when plotted on fig. 2. The ophitic group with a small range in Mg ratio (75–68) is similar to those found in the dominantly ophitic and intergranular Site 425 basalts and becomes rapidly depleted in Ca ($Ca_{40-20}$). Significantly compositions become more subcalcic close to plagioclase laths.

The granular pyroxenes have compositions more typical of those encountered amongst other Site 424 ferrobasalts. But they have a wider range of Mg ratio (65–30) with a relatively small variation in Ca. It is perhaps significant that the only ferropigeonite grain found in the mesostasis (Table I, anal. 11) is significantly poor in Al and Ti. As it is associated with skeletal plagioclase, this suggests

TABLE I. *Phenocryst and groundmass pyroxenes*

| | 1 | 2 | 3 | 4 | 5 | 6 | 7 | 8 | 9 | 10 | 11 |
|---|---|---|---|---|---|---|---|---|---|---|---|
| $SiO_2$ | 52.78 | 54.63 | 52.43 | 52.62 | 55.30 | 52.22 | 49.45 | 49.44 | 48.04 | 48.75 | 47.85 |
| $TiO_2$ | 0.37 | 0.26 | 0.41 | 0.35 | 0.20 | 0.44 | 1.46 | 1.00 | 1.85 | 0.96 | 0.89 |
| $Al_2O_3$ | 3.05 | 1.43 | 2.15 | 1.57 | 1.19 | 3.16 | 4.16 | 1.45 | 2.52 | 1.90 | 1.93 |
| $Cr_2O_3$ | 1.18 | 0.45 | 0.28 | 0.25 | — | 0.27 | 0.18 | — | 0.13 | — | — |
| FeO* | 5.14 | 7.37 | 8.32 | 8.61 | 13.60 | 7.06 | 11.07 | 22.78 | 22.52 | 27.65 | 26.01 |
| MnO | — | 0.19 | 0.17 | 0.15 | 0.31 | 0.22 | 0.15 | 0.54 | 0.51 | 0.54 | 0.39 |
| MgO | 16.66 | 20.72 | 17.05 | 17.95 | 23.97 | 16.36 | 13.42 | 9.18 | 8.56 | 6.51 | 14.55 |
| CaO | 21.20 | 15.21 | 18.47 | 16.79 | 6.17 | 20.07 | 19.67 | 15.74 | 15.99 | 14.52 | 7.64 |
| Rest | 0.13 | — | 0.49 | 0.39 | 0.15 | — | 0.78 | 0.24 | — | — | 0.59 |
| Total | 100.51 | 100.26 | 99.79 | 98.68 | 100.89 | 99.80 | 100.32 | 100.37 | 100.13 | 100.84 | 99.85 |
| Composition at % CaMgFe | | | | | | | | | | | |
| Ca | 43.8 | 30.6 | 37.9 | 34.6 | 12.3 | 41.5 | 41.9 | 34.0 | 35.2 | 32.2 | 15.9 |
| Mg | 47.9 | 57.9 | 48.7 | 51.5 | 66.5 | 47.1 | 39.7 | 27.6 | 26.2 | 20.0 | 42.0 |
| Fe | 8.3 | 11.6 | 13.4 | 13.9 | 21.2 | 11.4 | 18.4 | 28.4 | 38.6 | 47.8 | 42.1 |
| Mg/(Mg+Fe) | 85.3 | 83.4 | 78.5 | 78.8 | 75.9 | 80.5 | 68.3 | 41.8 | 40.4 | 29.5 | 49.9 |

1. Phenocryst Core, Site 425: endiopside section 425-8-1, piece 12.
2. Phenocryst Rim, from phenocryst in same thin section as 1.
3. Phenocryst Core, Site 424B, section 424B-6-1, piece 3.
4. Phenocryst Rim, same crystal as 3.
5. Groundmass Mg pigeonite: ophitic Site 425; 425-7-1, piece 7.
6. Groundmass, ophitic augite Site 425; 425-8-1, piece 14.
7. Groundmass, ophitic augite Site 424; 424-5-4, piece 1.
8. Groundmass; granular ferroaugite in mesostasis; same section as 7.
9. Groundmass, feathery pyroxene in glassy region Site 424; 424-6-1, piece 10c.
10. Groundmass, feathery pyroxene, edge of same crystal. Site 424.
11. Subcalcic Ferropigeonite in glassy mesostasis. Site 424; 424-6-1, piece 10b.

* Total iron calculated as FeO.

*Note.* A fuller selection of analyses is given by Mattey and Muir (1980). Others can be obtained from the authors.

that it nucleated from a liquid just depleted in Ca and Al, and crystallized before diffusion could restore the liquid composition.

Thus the pyroxene fractionation paths encountered in these rocks seem to be greatly influenced by the textures developed. The Site 425 basalt pyroxenes, which are relatively coarse grained, become progressively more subcalcic and may even develop pigeonite in immediate contact with plagioclase, while in the ferrobasalts with their quench textures the pyroxenes show clear evidence of a rise in Ca content as they enter the glassy areas (fig. 2); this is then followed by a late stage of very strong Fe enrichment.

Late-stage liquid immiscibility has been observed in the ferrobasalts. Here the silica-rich liquids as determined by broad-beam microprobe analyses (Foder *et al.*, 1980) are very poor in $K_2O$ as indeed were those which Dixon and Rutherford (1979) produced experimentally in crystallizing a primitive GSC basalt. Textures in these areas suggest that the crystalline phases now present are devitrification products of the original high-silica glass. The complementary Fe-rich liquid appears to have persisted for a much shorter time. It is represented now by the strongly Fe-enriched ferroaugites of the mesostasis, by thin sodic margins to the plagioclase, and by the abundant skeletal titanomagnetite crystals, some of which when probed contain nearly 24% $TiO_2$.

## *Conclusions*

We have seen that in metastable crystallization of clinopyroxenes, textural relations can influence the local composition of the melt and if the viscosity is high, or if crystal growth is very rapid, they can affect the compositions of the pyroxenes that separate. In the GSC ferrobasalts of Site 424 the trend towards Fe enrichment, initially produced by the widespread crystallization of plagioclase that depleted the melt in Ca and Al, was followed by the development of very Fe-rich ferroaugites produced by the demise of the silica-poor immiscible liquid.

High degrees of undercooling appear to promote rapid metastable crystallization of pyroxenes, probably at first by continued growth on to existing crystals which become increasingly subcalcic, rather than by developing new crystal nuclei. But at a later stage subcalcic pyroxenes also form in the groundmass, often accompanied by a minor amount of pigeonite. This process is well shown by some of the Hawaiian lavas with augite phenocrysts (Muir and Tilley, 1957; Fodor and Keil, 1975). The reverse trend from pigeonite towards subcalcic augite is also shown, with a reduced miscibility gap, by Hawaiian lavas that carry hypersthene phenocrysts (Muir and Long, 1965).

But metastable crystallization can also occur under plutonic conditions as was shown by Nwe's (1975) very careful study of the Skaergaard intercumulus pyroxenes of the trough bands in Upper Zone 'a'. The cumulus trend as determined by her probe analyses follows closely that established by Brown and Vincent (1963) for the ferroaugites. Their Ca-poor pyroxene trend as amended and extended by inclusion of more recent probe data, is shown in fig. 1. The intercumulus trend reveals a marked narrowing of the miscibility gap, together with a great enrichment in Fe. Fractionation here apparently took place under supersaturated and very tranquil conditions in small isolated cells, each of which appears to have behaved differently. Moreover, it now seems likely that liquid immiscibility may have contributed to the late stage of extreme Fe enrichment revealed by Nwe's analyses. Undercooling here has resulted locally in the development of the 'quench trend', unusual in a slowly cooled plutonic environment. In fig. 1 it can be compared with the equilibrium trend.

The varying behaviour of pyroxene crystallization under metastable conditions can be illustrated by means of a hypothetical pseudobinary phase diagram for the system $(Mg,Fe)_2SiO_6$–$Ca(Mg,Fe)Si_2O_6$ adapted from Yamakawa (1971). This is shown in fig. 3*a*. The initial composition of the liquid from which augite crystallizes is $L_1$. Under equilibrium conditions the composition of the liquid will change from $L_1$ to $L_2$ down the augite liquidus as the temperature decreases from $T_1$ to $T_2$. At $T_2$ pigeonite of composition $P_2$ will join augite $A_2$.

With more rapid cooling nucleation of pigeonite may be delayed, but the liquid in contact with augite $A_2$ will continue to precipitate an augite phase whose composition is determined by the metastable extension of the solidus. By temperature $T_3$ the augite composition will reach $A_3$ while the liquid composition is $L_3$. Hence the composition of the augite phase will become subcalcic. If the liquid progresses beyond $L_4$ it will become supersaturated with respect to pigeonite which will then appear in the groundmass. This situation is found in some Hawaiian lavas with augite phenocrysts.

With a slower cooling rate the system may still crystallize metastably but now under nearly isothermal conditions, and crystallization is likely to be dominated by parameters such as variation in the nucleation and growth-rate with temperature. In particular the establishment of a large number of successful nuclei is likely to be deferred; this can be represented approximately by nucleation curves drawn parallel to the liquidi (Gordon, 1968).

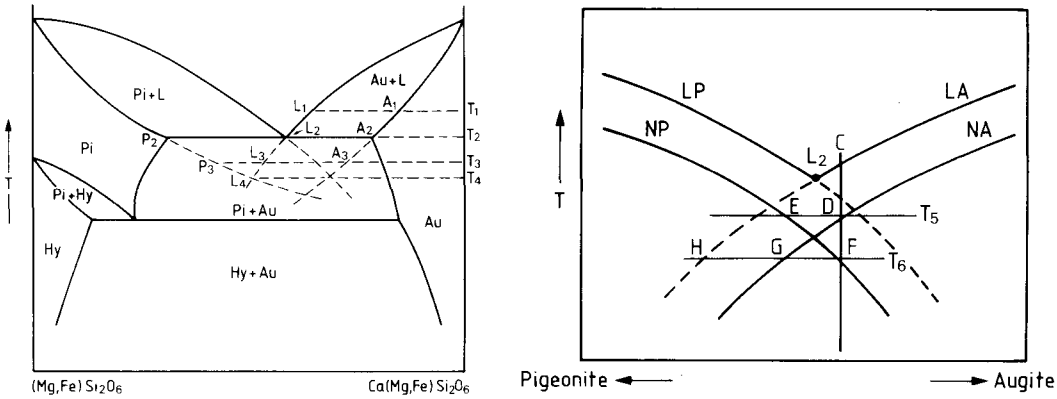


FIG. 3 (*a*, *left*). Hypothetical pseudobinary phase diagram to model crystallization of pyroxenes from tholeiitic magmas under metastable conditions. For details of sequences see text. (*b*, *right*). Enlargement of central part of liquidus curves of fig. 3*a* to show effects of supersaturated crystallization under nearly isothermal conditions. LA liquidus augite, LP liquidus pigeonite, NA nucleation curve augite, NP nucleation curve pigeonite. Crystallization sequences for T5 and T6 are discussed in the text.

Relations in the central portion of fig. 3*a* are illustrated in part in enlarged form in fig. 3*b*. Here augite and pigeonite are stable below their respective liquidus curves *LA* and *LP*, but effective nucleation of these phases will only set in when the temperature reaches the curves *NA* or *NP*. Nevertheless, individual crystals of augite or pigeonite under supercooled conditions will still remain stable at temperatures beneath the metastable extensions of their respective liquidus curves.

A slowly cooling melt of composition *C* will begin to nucleate substantial amounts of subcalcic augite when it reaches the point *D* at temperature $T_5$. But crystallization of the subcalcic pyroxene will change the composition of the liquid along the line *DE*. In this type of crystallization the composition of the melt will vary more than its temperature. Nucleation of subcalcic augite will virtually stop when the liquid leaves point *D*, but crystals already formed will still continue to grow. Eventually when the liquid reaches *E* it will be supersaturated with pigeonite and this may grow epitaxially on the subcalcic augite nuclei, or develop in favourable orientations on sector-zoned crystals. Alternatively, it may appear separately as groundmass grains.

Relations with distinctly higher degrees of supercooling are illustrated by the line at $T_6$. Conditions here are considered to be very quiescent so that phases will only nucleate homogeneously some distance below curves *NA* and *NP* respectively. In this case subcalcic augite would appear at *F* and pigeonite when the liquid reaches *G*. If the augite phase is the easier one to nucleate, which usually seems to be the case, the liquid may even reach *H* where any growth of augite nuclei should cease but pigeonite should crystallize easily. Hence a number of minor variations in crystallization sequences or in zoning compositions may arise in response to the degree of supercooling. Such considerations may partly explain the extraordinary oscillatory zoning described by Nwe in Cell 14 from a trough band of the Skaergaard Intrusion, and with greatly enhanced diffusion, could account for some of the fine 'loop the loop' oscillations described in the Apollo 12 pyroxenes by Boyd and Smith (1971).

A similar mechanism to this has been invoked by Maaløe (1978) to explain rhythmic layering sequences.

The Thingmuli trend can now be re-examined. Thingmuli was a large central volcano presumably fed from one or more small magma chambers. Analogies with two early stages in the differentiation can be seen if the average compositions of the Sites 424 and 425 phenocrysts are plotted on fig. 1. These approximately follow the Skaergaard trend, but their large field of scatter is almost certainly due to some of them not being true phenocrysts (Thompson and Humphris, 1980). If at different stages in an evolving magma there are successive eruptions of partly crystalline melt, the phenocrysts should define the equilibrium trend as determined by the appropriate intersection of the solidus with the solvus. But at each stage the groundmass compositions initially will follow the quench trend, reducing the miscibility gap, each step closing with a period of strong Fe enrichment as can be seen by examining Carmichael (1967, fig. 4).

The quench trend as outlined by Muir and Tilley

(1964) was indeed conceived with Kilauean and Japanese examples much in mind. Both trends are well shown in the Makaopuhi prehistoric lava lake 225 ft thick (Evans and Moore, 1968) where strong zoning and a wide scatter of compositions marks the chilled zone, but equilibrium crystallization with distinct Fe enrichment is seen in the slower-cooled parts.

In the thick Kilauean lavas of the modern summit and rift zone eruptions a similar scatter of compositions can be observed (Evans and Moore, 1968, fig. 8) but Fe enrichment following the Thingmuli pattern is rarely seen. These eruptions are fed by magma chambers continually replenished with more primitive magmas so that the compositions of successively erupted lavas are buffered against profound change (Wright and Fiske, 1971) and it is gas-charged oxygenated magma that is erupted. This precipitates titanomagnetite at a moderately late stage of crystallization and reduces the effect of the final stage of Fe enrichment in the pyroxenes. Only when fractionation can occur under conditions of low $f_{O_2}$ will strong Fe enrichment set in as in the schlier described by Kuno *et al.* (1957). For this reason the quench trend predominates in the pyroxenes of Kilauean lavas.

## REFERENCES


Barberi, F., Borsi, S., Ferrara, G., Marinelli, G., and Varet, J. (1970) *Phil. Trans. R. Soc. London*, Ser. A, **267,** 293–311.

——Bizouard, H., and Varet, J. (1971) *Contrib. Mineral. Petrol.* **33,** 93–107.

Boyd, F. R., and Smith, D. (1971) *J. Petrol.* **12,** 439–64.

Brown, G. M. (1957) *Mineral. Mag.* **31,** 511–43.

——and Vincent, E. A. (1963) *J. Petrol.* **4,** 175–97.

Carmichael, I. S. E. (1967) *Am. Mineral.* **52,** 1815–41.

Dixon, S., and Rutherford, M. J. (1979) *Earth Planet. Sci. Lett.* **45,** 45–60.

Evans, E. W., and Moore, J. G. (1968) *Contrib. Mineral. Petrol.* **17,** 85–115.

Fodor, R. V., and Keil, K. (1975) Ibid. **50,** 173–95.

——Berkley, J. L., Keil, K., Husler, J. W., Ma, M. S., and Schmidt, R. A. (1980) *Init. Rep. DSDP*, **54,** 737–50.

Gay, P., Bown, M. G., and Muir, I. D. with Bancroft, G. M., and Williams, P. G. L. (1971) *Proc. 2nd Lunar Sci. Conf.* **1,** 377–92.

Gordon, P. (1968) *Principles of Phase Diagrams in Materials Systems.* McGraw Hill, New York, 232 pp.

Hollister, L. S., and Gancanz, A. J. (1971) *Am. Mineral.* **56,** 959–79.

Kuno, H., Yamasaki, K., Iida, C., and Nagashima, K. (1957) *Jap. J. Geol. Geogr.* **27,** 179–218.

Maaløe, S. (1978) *Mineral. Mag.* **42,** 337–45.

McDougall, I. (1962) *Geol. Soc. Am. Bull.* **73,** 279–315.

Mattey, D. A., and Muir, I. D. (1980) *Init. Rep. DSDP*, **54,** 755–71.

Muir, I. D. (1954) *Mineral. Mag.* **30,** 376–88.

——and Long, J. V. P. (1965) Ibid. **34,** 358–69.

——and Tilley, C. E. (1957) *Am. J. Sci.* **255,** 241–53.

————(1964) *Geol. J.* **4,** 143–56.

Murase, T., and McBirney, A. R. (1970) *Science*, **167,** 1491–3.

Nakamura, Y. (1973) *Am. Mineral.* **58,** 986–90.

——and Kushiro, I. (1970) *Contrib. Mineral. Petrol.* **26,** 265–75.

Nwe, Y. Y. (1973) Ibid. **49,** 285–300.

Prewitt, C. T., Papike, J. J., and Bence, A. E. (1970) *Trans. AGU Supplement*, **51.**

Smith, P., and Lindsley, D. H. (1971) *Am. Mineral.* **58,** 225–33.

Thompson, R. N., and Humphris, S. E. (1980) *Init. Rep. DSDP*, **54,** 651–69.

Wager, L. R., and Deer, W. A. (1939) *Meddels. Grønland*, **105,** 1–352.

Wright, T. L., and Fiske, R. S. (1971) *J. Petrol.* **12,** 1–65.

Yamakawa, M. (1971) *Contrib. Mineral. Petrol.* **33,** 232–8.